

Explicit consideration of plant xylem hydraulic transport improves the simulation of crop response to atmospheric dryness in the US Corn Belt

Yi Yang^{1,2}, Kaiyu Guan¹, Bin Peng¹, Yanlan Liu^{3,4}, and Ming Pan⁴

¹Agroecosystem Sustainability Center, Institute for Sustainability, Energy, and Environment, University of Illinois at Urbana Champaign, Urbana, IL 61801, USA

²College of Agricultural, Consumer and Environmental Sciences, University of Illinois Urbana Champaign, Urbana, Illinois, USA

³School of Earth Sciences, Ohio State University

⁴Scripps Institution of Oceanography, University of California San Diego

November 3, 2023

1 Explicit consideration of plant xylem hydraulic transport improves
2 the simulation of crop response to atmospheric dryness in the US
3 Corn Belt

4

5 Yi Yang^{1,2*}, Kaiyu Guan^{1,2,3*}, Bin Peng^{1,2,3}, Yanlan Liu⁴, Ming Pan⁵

6

7 ¹Agroecosystem Sustainability Center, Institute for Sustainability, Energy, and Environment,
8 University of Illinois at Urbana Champaign, Urbana, IL 61801, USA

9 ²College of Agricultural, Consumer and Environmental Sciences, University of Illinois Urbana
10 Champaign, Urbana, Illinois, USA

11 ³National Center for Supercomputing Applications, University of Illinois Urbana Champaign,
12 Urbana, Illinois, USA

13 ⁴School of Earth Sciences, the Ohio State University, Columbus, Ohio, USA

14 ⁵Scripps Institution of Oceanography, University of California San Diego, La Jolla, California,
15 USA

16

17 *Corresponding authors: Yi Yang (yiy12@illinois.edu), Kaiyu Guan (kaiyug@illinois.edu)

18

19 **Abstract**

20

21 Atmospheric dryness (i.e., high vapor pressure deficit, VPD), together with soil moisture stress,
22 limits plant photosynthesis and threatens ecosystem functioning. Regions where rainfall and soil
23 moisture are relatively sufficient, such as the rainfed part of the U.S. Corn Belt, are especially
24 prone to high VPD stress. With globally projected rising VPD under climate change, it is crucial
25 to understand, simulate, and manage its negative impacts on agricultural ecosystems. However,
26 most existing models simulating crop response to VPD are highly empirical and insufficient in
27 capturing plant response to high VPD, and improved modeling approaches are urgently required.
28 In this study, by leveraging recent advances in plant hydraulic theory, we demonstrate that the
29 widely used coupled photosynthesis-stomatal conductance models alone are insufficient and
30 underestimate VPD stress effects on stomatal conductance and transpiration. Incorporating plant
31 xylem hydraulic transport significantly improves the simulation of transpiration under high VPD,
32 even when soil moisture is sufficient. Our results indicate that the limited water transport
33 capability from the plant root to the leaf stoma could be a major mechanism of plant response to
34 high VPD stress. We then introduce a Demand-side Hydraulic Limitation Factor (DHLF) that
35 simplifies the xylem and the leaf segments of the plant hydraulic model to only one parameter
36 yet captures the effect of plant hydraulic transport on transpiration response to high VPD with
37 similar accuracy. We expect the improved understanding and modeling of crop response to high
38 VPD to help contribute to better management and adaptation of agricultural systems in a
39 changing climate.

40

41 **1. Introduction**

42 Ecosystems, including agricultural ecosystems for food production, are prone to drought.
43 Drought adversely affects ecosystem functioning and reduces its productivity and crop yield
44 (Dietz et al., 2021; Y. Li et al., 2009). For many years, agricultural drought has been
45 characterized mostly by precipitation shortage and insufficient soil moisture (Alley, 1984;
46 Mishra & Singh, 2010; Palmer, 1965). Recent studies have demonstrated the increasing
47 importance of the adverse effects of atmospheric dryness (high vapor pressure deficit, VPD) on
48 ecosystem productivity, especially for regions where rainfall and soil moisture are relatively
49 abundant (Grossiord et al., 2020; Kimm et al., 2020; Kimberly A. Novick et al., 2016). The U.S.
50 Corn Belt located in the relatively humid Midwestern U.S., which is the world’s largest maize
51 and soybean production region, is primarily affected by atmospheric dryness stress compared to
52 soil moisture stress (Kimm et al., 2020). Moreover, VPD is projected to increase globally with
53 increasing temperature under climate change (IPCC Climate Change, 2013). The modeling and
54 understanding of crop response to VPD stress will be increasingly important to any mitigation or
55 adaptation strategies to ensure food production.

56

57 However, modeling plant water stress is a major challenge in land surface models, often causing
58 large uncertainties in simulated ecosystem energy, water, and carbon fluxes (Paschalis et al.,
59 2020; Rogers et al., 2017; Trugman et al., 2018). In modern land surface models, a coupled
60 photosynthesis-stomatal conductance model (Ball et al., 1987; Leuning, 1995; Medlyn et al.,
61 2011) combined with a module (Feddes et al., 1976; Sinclair et al., 1984; Venturas et al., 2017)
62 accounting for the effects of plant hydraulic transport on leaf gas exchange is typically used to
63 simulate stomatal conductance and transpiration. The dedicated scheme can be highly empirical
64 (e.g., the empirical soil water stress function, a.k.a., the beta function) or more mechanistic (plant
65 hydraulic models, PHM). Prior studies have demonstrated that despite the coupled-
66 photosynthesis stomatal conductance model capturing part of transpiration response to VPD
67 stress, plant hydraulic transport imposes additional limitations on stomatal conductance under
68 high VPD (Grossiord et al., 2020; Hubbard et al., 2001; Liu et al., 2020; Oren et al., 1999).
69 Meanwhile, the widely used empirical soil water stress function in current-gen and previous-gen

70 land surface and crop models does not respond to VPD. As a result, the simulation of
71 transpiration response to high VPD stress in many models bears large uncertainties.

72

73 Recent advances in plant hydraulic theory and modeling led to the wide incorporation of plant
74 hydraulic transport processes into many land surface models, resulting in better simulations of
75 plant response to water stress overall. Prior studies also demonstrated that PHMs can accentuate
76 the effect of VPD stress (Liu et al., 2020), underlining the necessity of PHMs to accurately
77 capture the full effects of VPD stress on ecosystem functioning, with empirical schemes being
78 mechanistically insufficient. However, to what extent plant hydraulic processes are important in
79 capturing VPD stress under different environmental conditions remains unclear, especially for
80 crops in rainfed regions where the primary water stress factor is VPD. Furthermore, although
81 PHMs provide more mechanistic representations and can theoretically achieve better accuracy, in
82 practice, PHMs have many parameters and are oftentimes difficult to measure and constrain
83 (Anderegg, 2015; Anderegg et al., 2018; Paschalis et al., 2020). This hinders the use of PHMs in
84 many cases where the observation data are scarce or have large uncertainties (Prentice et al.,
85 2015). Therefore, a more comprehensive assessment of the role plant hydraulic processes play in
86 crop response to VPD stress and a simplified representation of the relevant processes would be
87 beneficial for cropland applications.

88

89 In this paper, we aim to assess the necessity of plant hydraulic processes in capturing crop
90 transpiration response to high VPD stress and propose a simplified representation of the relevant
91 processes for easier applications. Specifically, we ask two questions: (1) To what extent are plant
92 hydraulic processes important in capturing VPD stress in the U.S. Corn Belt? (2) Is there room
93 for a simplified representation of the plant hydraulic model for simulating crop response to VPD
94 for improved efficiency in model simulation and parameter estimation? To answer the questions,
95 we first do numerical experiments to analyze the theoretical relationship between plant hydraulic
96 processes and the response to high VPD; then we conduct modeling experiments in flux tower
97 sites and compare model simulation with flux tower observations to assess the improvements of
98 incorporating PHM for capturing VPD stress; finally, we introduce a simplified method for
99 simulating VPD stress and demonstrate its effectiveness and efficiency. We expect the improved

100 understanding of the role of plant hydraulics in the response to VPD stress and the simplified
101 modeling method would contribute to better evaluation and management of agricultural drought
102 under a changing climate.

103

104

105 **2. Materials and Methods**

106 **2.1 Modeling of crop transpiration response to VPD**

107 **2.1.1 Coupled photosynthesis-stomatal conductance model**

108 In modern land surface models, plant transpiration response to water stress is jointly simulated
109 by a coupled photosynthesis-stomatal conductance model and a dedicated scheme to account for
110 water transport in the Soil-Plant-Atmosphere Continuum (SPAC). The response to VPD stress is
111 partially accounted for by the coupled photosynthesis-stomatal conductance model. The widely
112 used Ball-Berry model (Ball et al., 1987) takes relative humidity, which is highly correlated with
113 VPD, as one of the essential environmental factors to determine stomatal conductance. Other
114 similar models such as the Ball-Berry-Leuning (Leuning, 1995) and Medlyn (Medlyn et al., 2011)
115 stomatal conductance models directly use VPD as an input. In all these models, stomatal
116 conductance reduces with rising VPD. In this study, we use the Medlyn stomatal conductance
117 model as stated by

$$118 \quad g_{s,NHL} = g_0 + \left(1 + \frac{g_1}{\sqrt{D}}\right) \frac{A}{C_a} \quad (1)$$

119 where $g_{s,NHL}$ is stomatal conductance (m s^{-1}) with no hydraulic limitation (NHL), g_0 and g_1 are
120 fitted parameters, D is VPD (Pa), A is net CO₂ assimilation rate ($\mu\text{mol m}^{-2} \text{s}^{-1}$), and C_a is
121 atmospheric CO₂ concentration ($\mu\text{mol mol}^{-1}$). We will continue using the subscript NHL
122 throughout the article to represent relevant variables that are calculated by the coupled
123 photosynthesis-stomatal conductance model without the constraint caused by plant hydraulic
124 transport in the SPAC, and we refer to the land surface model configured without the constraint
125 of plant hydraulic transport as the NHL model.

126

127 **2.1.2 Plant hydraulic model**

128 Mechanistically, water transport in the SPAC also responds to VPD and can constrain
 129 transpiration when the water transport capability is limited under high VPD (fig. 1b). Many
 130 current-generation land surface models use process-based plant hydraulic models as a
 131 mechanistic scheme to simulate water transport. Previously, highly empirical schemes such as
 132 the empirical soil water stress function and the supply-demand balance scheme were used as an
 133 approximation of the constraint of water transport on transpiration. Recent advances in modeling
 134 plant response to water stress further demonstrated that the empirical schemes are special cases
 135 of the mechanistic plant hydraulic models under certain conditions (Yang et al., 2023)¹. Notably,
 136 the widely used empirical soil water stress function does not respond to VPD and hence
 137 inherently unable to capture water transport limitation in response to VPD stress.

138

139 In this study, we use a three-segment plant hydraulic model (fig. 1a) to simulate water transport
 140 in the SPAC (L. Li et al., 2021). Water transport from the soil to the root xylem and from the
 141 root xylem to the leaf is driven by water potential differences and controlled by rhizosphere and
 142 xylem conductances.

$$143 \quad Q_{sx} = g_{sx}(\psi_s) \cdot (\psi_s - \psi_{rx} - h_s) \quad (2)$$

$$144 \quad Q_{xl} = g_{xl}((\psi_{rx} + \psi_l)/2) \cdot (\psi_{rx} - \psi_l - h_c) \quad (3)$$

145 where Q_{sx} and Q_{xl} are the water flow from the soil to the root xylem and from the root xylem to
 146 the leaf, respectively; g_{sx} and g_{xl} are the respective conductances; ψ_s , ψ_{rx} and ψ_l are soil, root
 147 xylem and leaf water potentials, respectively; and h_s and h_c are soil layer depth and canopy
 148 height. In this work, instead of calculating water flow from many soil layers, we use the effective
 149 root zone depth for Midwestern crops for simplicity. We also use the average of root xylem and
 150 leaf water potentials for the calculation of xylem water potential to account for the gradual
 151 decline of water potential from the root xylem to the leaf. The rhizosphere conductance is
 152 determined by root and soil hydraulic properties, and we use a cylindrical root model (Manzoni
 153 et al., 2013) and the Brooks-Corey soil hydraulic model to calculate it:

$$154 \quad g_{sx}(\psi_s) = \sqrt{RAI}/(\pi d) \cdot K_{sat} \cdot (\psi_s/\psi_{s,sat})^{-2-3/b} \quad (4)$$

¹ Yang, Y. (2023). A unified framework to reconcile theories of modeling transpiration response to drought: plant hydraulics, supply-demand balance, and empirical soil water stress. Manuscript submitted for publication.

155 where RAI is the root area index, d is the root zone layer depth, K_{sat} is saturated soil hydraulic
 156 conductivity, ψ_s is soil matric potential, $\psi_{s,sat}$ is saturated soil matric potential, and b is the soil
 157 particle size distribution parameter. We use a sigmoid function to parametrize xylem
 158 vulnerability curve:

$$159 \quad g_{xl}(\psi_x) = g_{xl,max} \cdot (1 + (\psi_x/\psi_{x,50})^{a_1})^{-1} \quad (5)$$

160 where $g_{xl,max}$ is maximum xylem conductance, $\psi_{x,50}$ is the xylem water potential at 50% loss of
 161 conductance and a_1 is a shape parameter. The stomatal response function to leaf water potential
 162 is also parameterized by a sigmoid function:

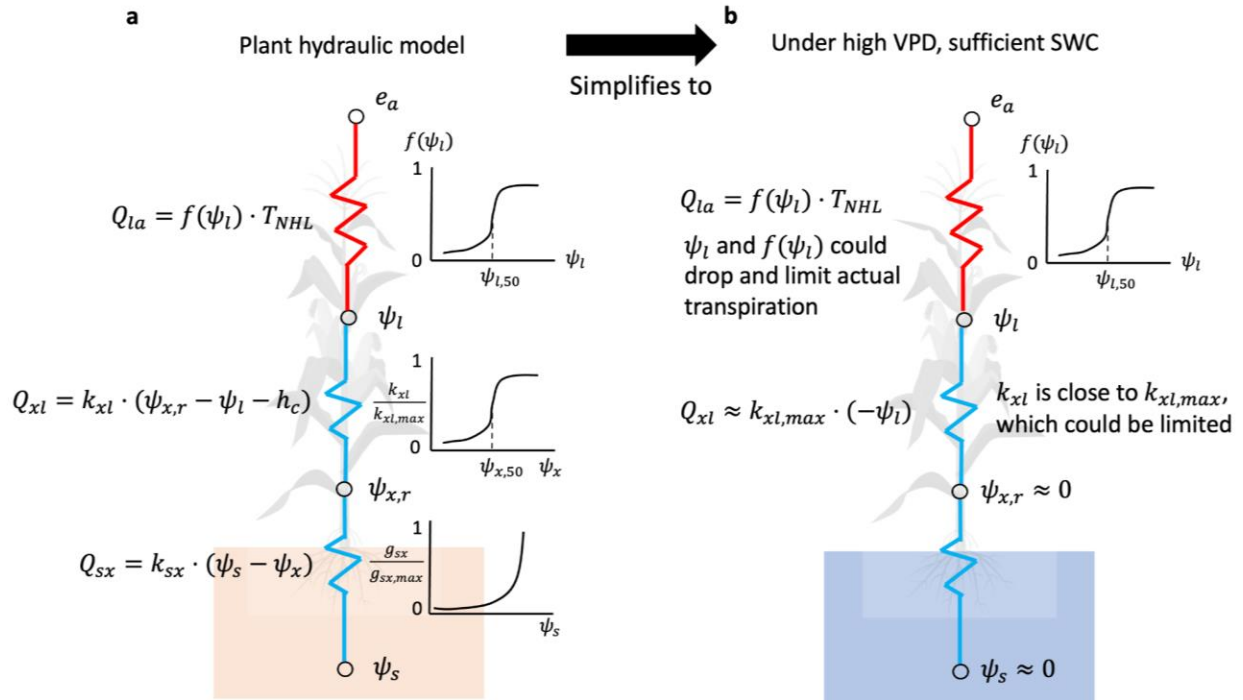
$$163 \quad f(\psi_l) = g_s(\psi_l)/g_{s,NHL} = (1 + (\psi_l/\psi_{l,50})^{a_2})^{-1} \quad (6)$$

164 where a_2 is a shape parameter, and $\psi_{l,50}$ is the leaf water potential at 50% loss of stomatal
 165 conductance compared with NHL conditions. The final stomatal conductance is the NHL
 166 conductance calculated by the coupled photosynthesis-stomatal conductance model multiplied by
 167 the stomatal response function, and the actual transpiration is

$$168 \quad T = T_{NHL} \cdot f(\psi_l) \quad (7)$$

169 The plant hydraulic model takes soil moisture and NHL transpiration T_{NHL} as input and is solved
 170 iteratively until water flows in every segment are equal:

$$171 \quad Q_{sx} = Q_{xl} = T \quad (8)$$



172

173 Fig. 1. Illustration of the plant hydraulic model (a) and how it affects plant response to VPD
 174 stress (b). The PHM is represented by the electric circuit analogy. On the left are the equations
 175 for water flow, and on the right are the functions for conductances. Under sufficient SWC (b),
 176 soil and root xylem water potentials are close to 0, and xylem conductance is close to the
 177 maximum conductance. However, leaf water potential could still drop significantly to overcome
 178 limited xylem conductance, and as a result stomatal may close in response to low leaf water
 179 potential and limit actual transpiration.

180

181 2.1.3 Radiation and turbulent transfers

182 We use the Noah-MP land surface model for the above-ground radiation and turbulent transfers
 183 (Niu et al., 2011; Z.-L. Yang et al., 2011). We choose Noah-MP for its wide usage in the
 184 meteorological and climate modeling communities and its computational efficiency. Readers are
 185 referred to (Niu et al., 2011; Z.-L. Yang et al., 2011) for a full description of the radiation and
 186 turbulent transfer schemes in Noah-MP. Relevant modules were extracted from the original
 187 Noah-MP model and coupled with the above-described stomatal conductance and plant hydraulic
 188 models. The full model is forced by meteorological data including air temperature, pressure,
 189 humidity, downward solar and longwave radiation, and precipitation. Because soil moisture

190 simulation is closely coupled with plant response to water stress (Lei et al., 2018), we use
191 measured soil moisture as input instead of simulating it to reduce uncertainties. In the full model,
192 the calculation of actual transpiration can be viewed as a two-step process: in the first step, the
193 coupled photosynthesis-stomatal conductance model, together with the radiation and turbulent
194 transfer schemes, resolves stomatal conductance and transpiration under the NHL conditions
195 ($g_{s,NHL}$ and T_{NHL} ; note, we use T to denote transpiration instead of temperature); in the second
196 step, the plant hydraulic model takes T_{NHL} and $g_{s,NHL}$ as input and downregulates transpiration
197 and stomatal conductance based on the water transport limitation in the SPAC and calculates the
198 actual transpiration T and stomatal conductance g_s (see Section 4 for the implications of the
199 two-step conceptualization). In this study, in addition to running the full model, we also conduct
200 numerical experiments of running the plant hydraulic model only to demonstrate the limitation
201 from plant hydraulic transport on transpiration under high VPD stress. In the plant hydraulic
202 model only experiment, soil moisture and the NHL transpiration are prescribed and provided as
203 input.

204

205

206 **2.2 Demand-side Hydraulic Limitation Factor (DHLF)**

207 Although plant hydraulic models provide the most complete mechanistic representations, they
208 are complex, have many parameters, and, oftentimes, difficult to measure and constrain. We here
209 derive a simplified method for simulating high VPD stress based on the plant hydraulic model.
210 First, since we only focus on VPD stress when soil moisture is sufficient, which is typically the
211 case for the rainfed region of the U.S. Corn Belt, the rhizosphere water transport segment can be
212 neglected; instead, the root xylem water potential can be approximated by zero, which is close to
213 the soil water potential when soil moisture is sufficient. The two remaining processes directly
214 controlling transpiration response to VPD (xylem water transport and stomatal response to leaf
215 water potential) have in total six parameters: $g_{xl,max}$, $\psi_{x,50}$, a_1 , h_c , $\psi_{l,50}$, and a_2 . In practice, as
216 in many process-based physical models, many parameters could be redundant if we only focus
217 on the final response. In this study, we only keep one parameter out of the six, the maximum
218 xylem conductance $g_{xl,max}$, and test if only keeping the one parameter can largely reproduce the
219 response of the original formulation. That is, we test if the effects on the final response (the

220 actual transpiration) of changing the other four parameters can be compensated by a
221 corresponding change of $g_{xl,max}$. Specifically, in the test, we first do a numerical analysis
222 similar to the plant hydraulic model only experiment mentioned in Section 2.1.3 by providing the
223 NHL transpiration T_{NHL} as input and check if the actual transpiration response T are the same
224 between the two formulations. We then test the two formulations using data from the flux tower
225 (Section 2.3) to evaluate the real-world performance of the simplified formulation. We call the
226 formulation with the only one adjustable parameter $g_{xl,max}$ to Demand-side Hydraulic
227 Limitation Factor (DHLF), where demand-side means it only pertains to the stress from
228 atmospheric dryness.

229

230

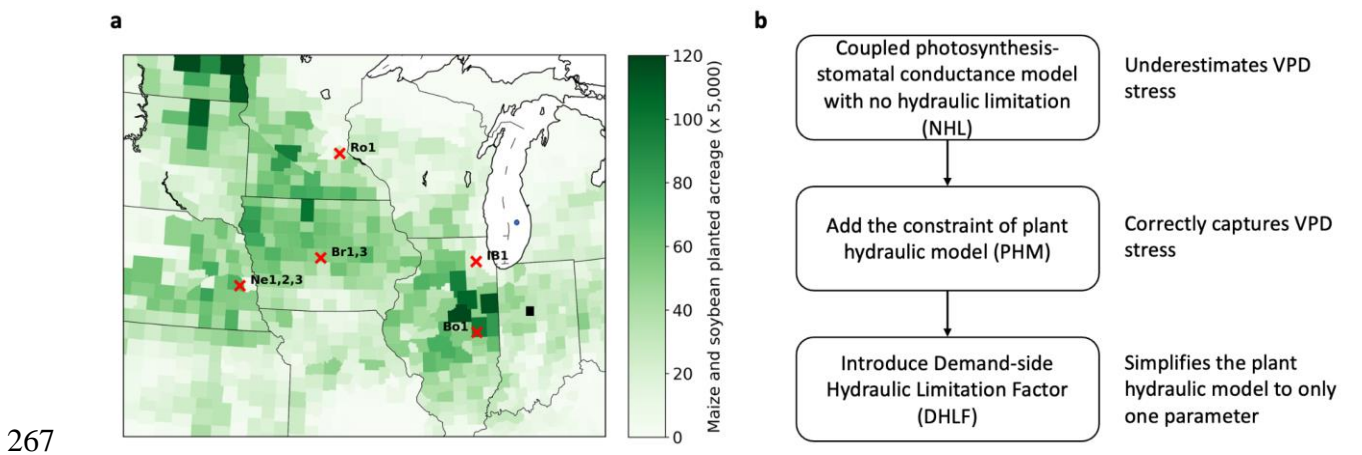
231 **2.3 Study region and experiment design**

232 We conducted the modeling experiments in seven flux tower sites located in the U.S. Corn Belt
233 (fig. 2a and table 2). Among them, US-Ne1 (Suyker, 2016a) and US-Ne2 (Suyker, 2016b) are
234 irrigated sites and other sites are rainfed. The meteorological forcings and soil moisture from the
235 flux towers are used to drive the model. For the three Ne sites (US-Ne1-3), the meteorological
236 forcings and ET data are from the FLUXNET2015 dataset (Baldocchi et al., 2001), and the soil
237 moisture data are from the Ameriflux dataset (K. A. Novick et al., 2018). For all other sites, all
238 measurements are from the Ameriflux dataset. For some sites (US-Br1, US-Br3, and US-Ro1)
239 where soil moisture measurements are only available at the surface depth (e.g., 0.05 cm), we use
240 the simulated root zone soil moisture from the full Noah-MP as a supplement (Y. Yang et al.,
241 2021). We use site-measured LAI for the three NE sites and satellite remote sensing LAI
242 estimates for other sites (Jiang et al., 2020; Y. Yang et al., 2021). Soil hydraulic parameters are
243 obtained from the gSSURGO soil database (Mitter, 2017). Model parameters related to plant
244 photosynthesis, stomatal conductance, and hydraulic transport are calibrated using the ET data
245 from the flux towers, with values from previous literature as the baseline. Since we primarily
246 focus on high VPD stress in this study, we calibrate and evaluate the model using midday ET
247 observations. We only evaluate the model during the peak growing season (7/1 to 8/15 for maize
248 and 7/15 to 9/1 for soybean) to minimize the effects caused by the uncertainties of simulated soil

249 evaporation. In addition, periods when model simulation indicates significant canopy or soil
250 evaporation are also excluded.

251

252 We first run the model with no hydraulic limitation and calibrate the most important
253 photosynthesis and stomatal conductance parameters (the maximum carboxylation rate V_{max} and
254 g_1) to achieve good performance when VPD is low (mid-day VPD is lower than 1000 Pa). We
255 then run the complete model with plant hydraulic components and calibrate five out of the six
256 plant hydraulic parameters (canopy height is excluded due to its clear physical meaning; site
257 measurement values are taken instead) related to VPD stress (rhizosphere related parameters are
258 fixed and not calibrated). We use the parameter values from the literature ([Kattge et al., 2009](#);
259 [Lin et al., 2015](#); [Miner et al., 2017](#); [Miner & Bauerle, 2019](#); [Sperry, 2000](#)) as the prior and only
260 allow them to change at most 20% from their prior values during the calibration to ensure they
261 do not deviate too much from previous research. All other parameters not included in the
262 calibration are from previous literature or the Noah-MP look up table. The performance of the
263 NHL model and the complete model are then compared to evaluate the importance of hydraulic
264 limitation in simulating transpiration response to VPD stress. Finally, we evaluate the
265 performance of the simplified DHLF formulation and compare it with the complete model with
266 the original plant hydraulic formulation.



268 Fig. 2. The study region and flux tower sites in the U.S. Corn Belt with county level maize and
269 soybean planted acreage in the background (a) and the workflow of the modeling experiments
270 (b).

271

272 Table 1. The parameters calibrated in the modeling experiment. The two parameters in the NHL
 273 formulation (coupled photosynthesis-stomatal conductance only) are first calibrated under low
 274 VPD conditions. The PHM and DHLF are then calibrated with the NHL parameters fixed to the
 275 calibrated values from the first step.

NHL (first step)	PHM (second step)	DHLF (second step)
V_{max} (maximum carboxylation rate)	$g_{xl,max}$ (maximum xylem conductance)	$g_{xl,max}$ (maximum xylem conductance)
g_1 (the Medlyn stomatal conductance model slope parameter)	$\psi_{x,50}$ (xylem water potential at 50% of conductance loss)	$\psi_{x,50}$ removed (xylem conductance fixed to the maximum)
	a_1 (xylem vulnerability curve shape parameter)	a_1 removed
	$\psi_{l,50}$ (leaf water potential at 50% stomatal conductance loss due to hydraulic limitation)	$\psi_{l,50}$ fixed to $-100 \text{ mH}_2\text{O}$
	a_2 (stomatal-leaf water potential response function shape parameter)	a_2 fixed to 6

276

277

278 Table 2. Information of the flux tower sites in the modeling experiments.

Site	Year	MAP/mm	MAT/°C	Rainfed/Irrigated	Crop type
US-Bo1	2000-2008	792.10	11.40	rainfed	Maize in odd years, soybean in even years
US-Br1	2005-2011	933.61	9.13	rainfed	odd maize,

						even soybean
US-IB1	2005-2011	966.76	9.52	rained		even maize, odd soybean
US-Ro1	2004-2012	762.45	7.71	rained		odd maize, even soybean
US-Br3	2005-2011	836.91	9.22	rained		even maize, odd soybean
US-Ne1	2003-2012	840.40	10.60	irrigated		continuous maize
US-Ne2	2003-2012	871.80	10.32	irrigated		odd maize even soybean before 2009, maize beginning 2009
US-Ne3	2003-2012	712.15	10.42	rained		odd maize, even soybean

279

280

281 3. Results

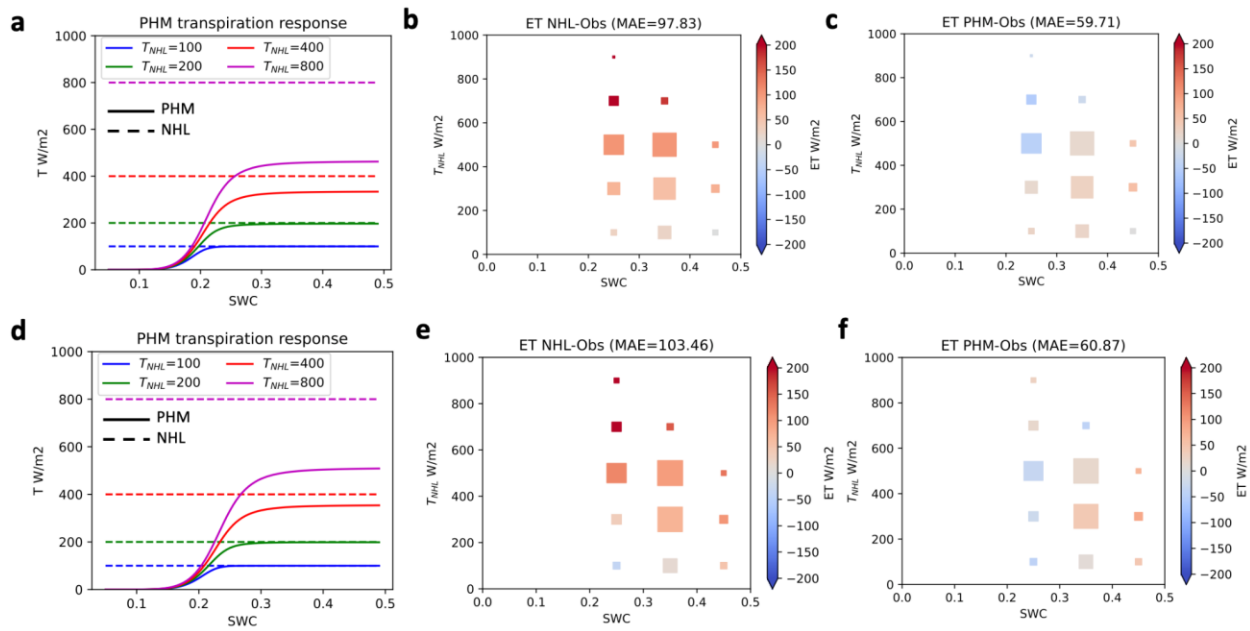
282 3.1 Incorporating plant hydraulic transport processes improves simulation of crop 283 response to VPD stress

284 In the numerical experiment of running the plant hydraulic model only, there is significant
285 transpiration downregulation when T_{NHL} is high even when SWC is sufficient (fig. 3).
286 Mechanistically, high atmospheric dryness increases T_{NHL} , and if the plant xylem hydraulic
287 conductance is limited, low leaf water potential is required to create sufficient water potential
288 gradient to drive xylem water transport. However, low leaf water potential also causes stomata to
289 close and limit transpiration. Note although stomatal conductance responds to high VPD
290 negatively in the stomatal conductance model, the NHL transpiration still increases.

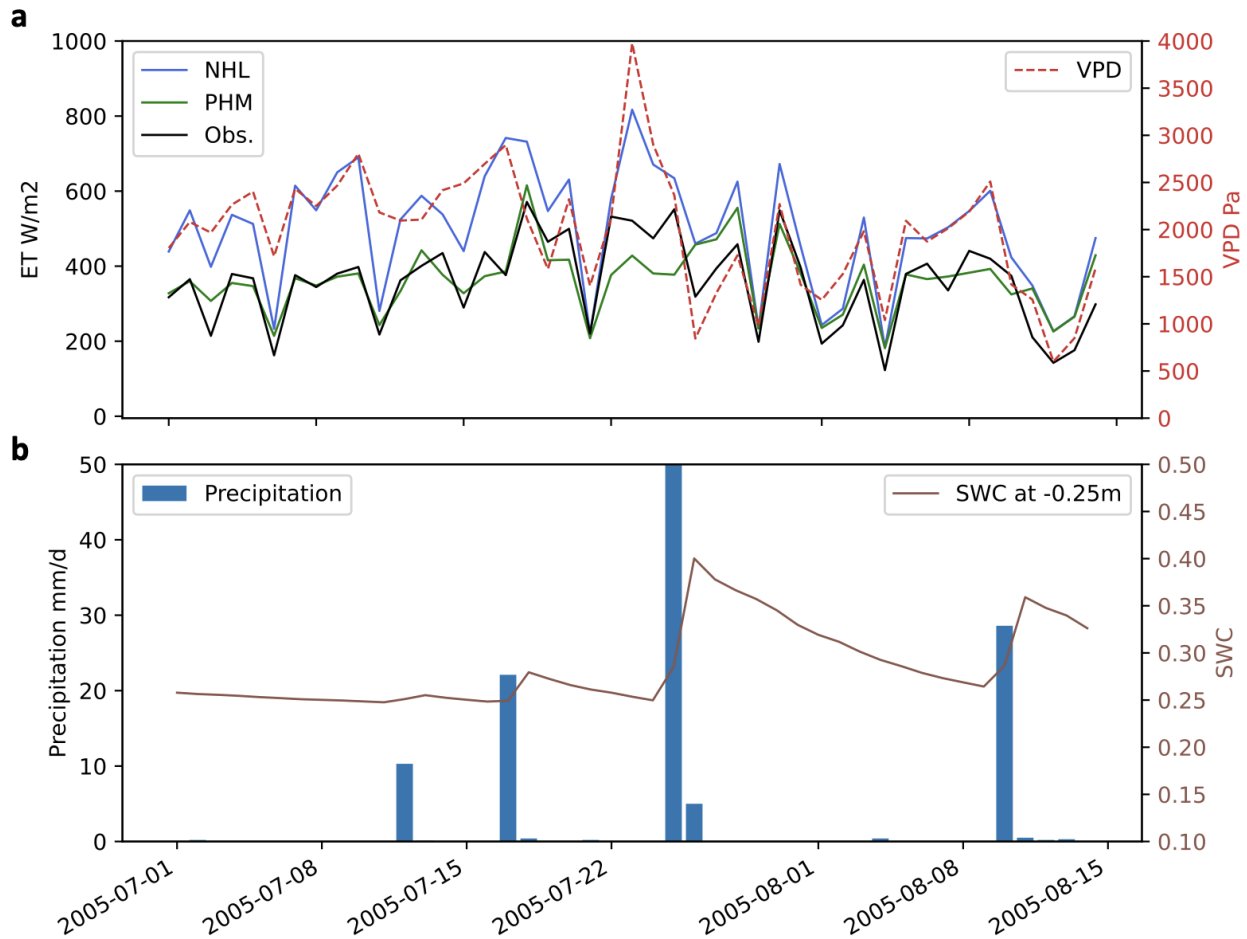
291

292 In the modeling experiments using flux tower data, for both maize and soybean, the NHL model
293 significantly overestimates ET during relatively dry years compared with flux tower
294 measurements. The overestimation mainly occurs when atmospheric dryness is high (T_{NHL} is

295 high) and increases when T_{NHL} increases (fig. 3). Incorporating the limitation from plant
 296 hydraulic transport largely corrects the overestimation, which indicates that stomatal
 297 conductance models alone, though also responds to VPD, are insufficient to capture high VPD
 298 stress. As indicated in the flux tower measured data, root zone soil moisture in these corn belt
 299 sites rarely drops below 0.25, even in an extreme drought year like 2012; as a result, soil
 300 moisture is not a significant limiting factor for crop transpiration (fig. S1). In fact, even in the
 301 extreme drought year of 2012 where soil moisture stress does play a role, high VPD stress is still
 302 the dominant stress factor. Detailed time series analysis (fig. 4) reveals that the NHL
 303 transpiration has the largest overestimation compared to flux tower observation when VPD is
 304 high; during the entire peak growing season, soil moisture at 0.25 m depth, which covers the
 305 upper fraction of the root zone, is almost always above 0.25.



306
 307 Fig. 3. **a**, The numerical experiments of the transpiration responses; the dashed horizontal lines
 308 are the NHL transpiration (NHL does not respond to soil water stress and underestimate VPD
 309 stress) and the solid lines are the transpiration response of the PHM. **b**, The bias of the simulated
 310 ET by models without hydraulic limitation; and **c**, with plant hydraulic processes evaluated with
 311 flux tower data for maize. The joint distribution of T_{NHL} and SWC is binned, and the square size
 312 represents the density of data in the binned region. Mean absolute errors (MAE) are given in the
 313 figure title. **d-f**, The same as **a-c** but for soybean.



315

316 Fig. 4. **a**, Time series of ET calculated with (PHM) and without (NHL) hydraulic transport
 317 limitation (NHL) compared with flux tower observed data (Obs.) for US-Ne3 in 2005; VPD is
 318 also shown. **b**, time series of precipitation and SWC at 0.25 m depth for the same period.

319

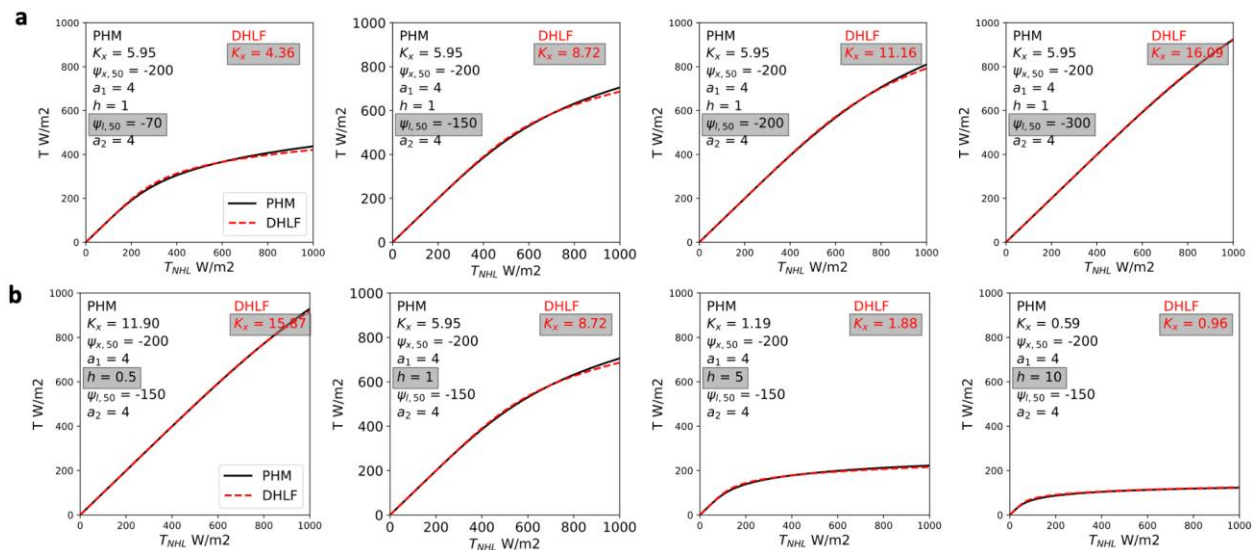
320 3.2 The effectiveness and efficiency of Demand-side Hydraulic Limitation Factor

321 In the numerical analysis, the DHLF formulation achieves nearly identical response as the
 322 original plant hydraulic model across realistic ranges of T_{NHL} (from 0 to $1000 W/m^2$) and the
 323 six plant hydraulic parameters (fig. 5 and fig. S2). The effects on the actual transpiration
 324 response of changes in other parameters can be compensated by an appropriate change of $g_{xl,max}$
 325 alone in the DHLF formulation. This indicates that the six parameters related to VPD stress in
 326 the original PHM are largely redundant in terms of calculating the final response of actual

327 transpiration and the simplified DHLF formulation is effective and more efficient. Specifically,
 328 DHLF captures the effects of changing h_c and $\psi_{l,50}$ accurately, showing little difference between
 329 the two formulations. $\psi_{l,50}$ and h_c are also the most important parameters in addition to $g_{xl,max}$,
 330 which is preserved by DHLF. There are slight differences between DHLF and the original PHM
 331 when $\psi_{x,50}$, a_1 , or a_2 are modified; however, the three parameters are relatively insignificant for
 332 capturing VPD response, and the two shape parameters are inherently empirical, and thus the
 333 differences can be considered minor.

334

335 Modeling experiments using flux tower data confirms the effectiveness of the DHLF formulation.
 336 The calibrated DHLF and original PHM have similar performance evaluated against flux tower
 337 ET observation (fig. 6**abde**). The responses between the two formulations are also similar if
 338 compared against each other (fig. 6**cf**); the minor differences between them are mainly caused by
 339 the presence of the response to soil moisture stress in the PHM, which is insignificant in the
 340 study region. A typical time series similar to fig. 4 is provided in fig. S3.

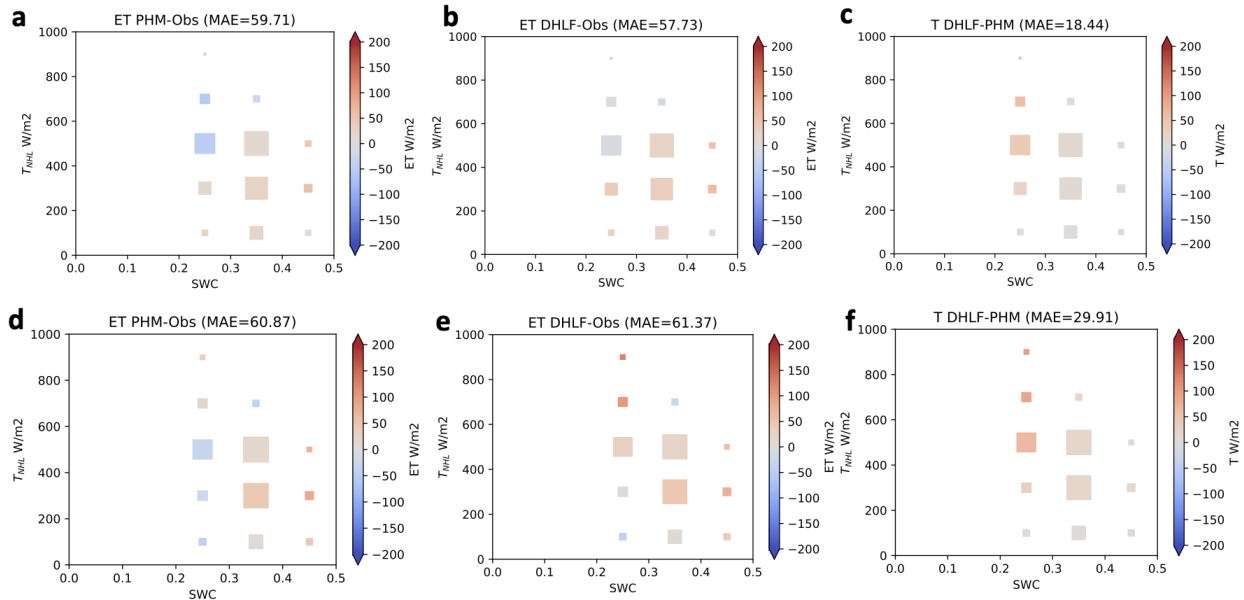


341

342 Fig. 5. The actual transpiration response of the DHLF formulation compared with the original
 343 PHM under sufficient SWC with T_{NHL} prescribed as input. **a**, change $\psi_{l,50}$ in the PHM and
 344 calibrate the only parameter ($g_{xl,max}$) in DHLF to match the response of PHM. **b**, change h_c in
 345 the PHM and calibrate DHLF to match the response. The parameters on the left are from the
 346 PHM (gray background denotes the parameter changed), and the parameter on the right is the

347 DHLF formulation. The solid black lines (PHM) and dashed red lines (DHLF) largely overlap.
348 For changes of other parameters in the PHM, please see fig. S2.

349



350

351 Fig. 6. The bias of the simulated ET by the original PHM (a) and the DHLF formulation (b)
352 evaluated with flux tower data, and the bias of the simulated transpiration by the DHLF
353 formulation evaluated against the original PHM for maize (c). The figure layout is the same as in
354 fig. 6bcef. d-f, the same as a-c but for soybean.

355

356 4. Discussion

357 Our modeling experiments demonstrate that plant hydraulic processes are important in capturing
358 high VPD stress in the U.S. Corn Belt. In the experiments, the NHL model configuration with
359 the coupled photosynthesis-stomatal conductance model alone severely overestimates crop
360 transpiration (underestimate VPD stress) under high VPD and incorporating plant hydraulic
361 transport processes significantly improves the simulation of transpiration. Previous studies have
362 shown that theoretically PHM accentuates the effect of VPD stress on transpiration regardless of
363 soil water status (Liu et al., 2020). Our study indicates that in regions where VPD stress is high
364 such as the Midwestern U.S., the widely used stomatal conductance model alone is insufficient
365 for capturing VPD stress, and thus the representation of plant hydraulics is necessary. Notably,

366 as some empirical schemes to represent water transport limitations, such as the empirical soil
367 water stress function (Feddes et al., 1976), do not respond to VPD, many land surface models
368 configured with these schemes will also be insufficient for capturing VPD stress. Therefore, we
369 argue that plant hydraulics would be beneficial to correctly simulating crop response to rising
370 VPD especially under future climate scenarios.

371

372 Our study also demonstrates that the PHM can be largely simplified for simulating transpiration
373 response to VPD stress. One major downside of PHM preventing its wide adoption is its
374 complexity and the large number of parameters. We here demonstrate that, specifically for the
375 response to VPD stress, the parameter space can be compressed with little to no sacrifice of
376 accuracy. The six parameters involved in the response to VPD stress can be simplified to one
377 parameter. Numerical model experiments show that the effects of changing other parameters can
378 be achieved by an appropriate change of the DHLF. Flux tower site testing further demonstrates
379 that the performance of the simplified DHLF formulation is similar to the original PHM in terms
380 of capturing the response to VPD stress. We envision that the DHLF method can be a useful tool
381 in improving the simulation of plant response to VPD stress in many cases where 1) the final
382 response is the main point of interest instead of detailed process understanding, 2) data
383 availability is limited, and therefore model parsimony is preferred.

384

385 Note that a few limitations exist in this analysis. First, there are two prerequisites to the
386 conclusion that the coupled photosynthesis-stomatal conductance alone is insufficient for
387 capturing high VPD stress in the U.S. Corn Belt: (1) the NHL model alone with parameters close
388 to literature values underestimates high VPD stress, and (2) the NHL model structure and
389 literature values of its parameters are largely correct. The second one is indispensable because
390 with the flux tower data only (atmospheric forcing and evapotranspiration measurements), the
391 coupled photosynthesis-stomatal conductance model alone can for certain match the flux tower
392 data with appropriate functional form and parameters (even if the widely used Medlyn or Ball-
393 Berry models cannot, a new functional form can be developed to match the data). To support the
394 conclusion without (2), more measurement data or experiments will be required, e.g., sap flow,
395 leaf water status. Second, the two-step formulation of sequentially running the NHL model and

396 the PHM is only one way of setting up a land surface model with plant hydraulic processes. We
397 choose this two-step formulation for its simplicity and ease of use, and we do not expect it to
398 significantly interfere with the main points of this study. The first point regarding the inadequacy
399 of the coupled photosynthesis-stomatal conductance for capturing VPD stress does not depend
400 on how the PHM is incorporated in the full model. For the second point regarding the
401 redundancy of PHM parameters, we do expect the exact results to be slightly different if a
402 different coupling method is used for the PHM, but we still expect the effect of hydraulic
403 constraint on transpiration to be similar on a first-order basis, and most importantly there is still
404 sufficient room for simplification.

405

406

407 **5. Conclusion**

408 In this study, through numerical experiments and site testing, we demonstrate that the widely
409 used coupled photosynthesis-stomatal conductance model alone is insufficient for simulating
410 crop transpiration response to VPD stress in the U.S. Corn Belt. Plant hydraulic transport
411 processes are required for correctly capturing crop response to VPD stress even under sufficient
412 soil moisture. We then introduce a simplified DHLF formulation derived from the plant
413 hydraulic model with only one parameter specifically for simulating the limitation of hydraulic
414 transport on transpiration. The simplified formulation achieves nearly the same response as the
415 original PHM and similar performance in flux tower site testing. We envision that the improved
416 understanding of the role that plant hydraulics plays in crop response to VPD and the simplified
417 modeling method would facilitate future research and applications in the management and
418 adaptation of agricultural ecosystems to a changing climate.

419

420 **Acknowledgement**

421 We acknowledge the support from NSF CAREER award (Award Abstract #1847334) managed
422 through the NSF Environmental Sustainability Program and USDA/NSF Cyber-Physical-System
423 Program. We acknowledge the support from USDA NIFA CPS project. We acknowledge the
424 following AmeriFlux sites for their data records: US-Ne1,US-Ne2,US-Ne3, US-Bo1, US-Br1,
425 US-IB1, US-Ro1, US-Br3. In addition, funding for AmeriFlux data resources and core site data
426 was provided by the U.S. Department of Energy's Office of Science.

427

428 **Open Research**

429 The data that support the findings of this study are available in Ameriflux at
430 <https://ameriflux.lbl.gov/> and other literature referenced in the manuscript. The code for
431 producing the analysis is available on Github via Zenodo (Frostbite7. (2023).
432 Frostbite7/crop_hydro: Preview version for investigating VPD stress on crops (preview). Zenodo.
433 <https://doi.org/10.5281/zenodo.8432287>).

434

435

436 **References:**

- 437 Alley, W. M. (1984). The Palmer Drought Severity Index: Limitations and Assumptions. *Journal*
438 *of Applied Meteorology and Climatology*, 23(7), 1100–1109.
- 439 Anderegg, W. R. L. (2015). Spatial and temporal variation in plant hydraulic traits and their
440 relevance for climate change impacts on vegetation. *The New Phytologist*, 205(3), 1008–
441 1014.
- 442 Anderegg, W. R. L., Konings, A. G., Trugman, A. T., Yu, K., Bowling, D. R., Gabbitas, R., et al.
443 (2018). Hydraulic diversity of forests regulates ecosystem resilience during drought.
444 *Nature*, 561(7724), 538–541.
- 445 Baldocchi, D., Falge, E., Gu, L., Olson, R., Hollinger, D., Running, S., et al. (2001). FLUXNET:
446 A New Tool to Study the Temporal and Spatial Variability of Ecosystem-Scale Carbon
447 Dioxide, Water Vapor, and Energy Flux Densities. *Bulletin of the American*
448 *Meteorological Society*, 82(11), 2415–2434.
- 449 Ball, J. T., Woodrow, I. E., & Berry, J. A. (1987). A Model Predicting Stomatal Conductance
450 and its Contribution to the Control of Photosynthesis under Different Environmental
451 Conditions. In J. Biggins (Ed.), *Progress in Photosynthesis Research: Volume 4*
452 *Proceedings of the VIIth International Congress on Photosynthesis Providence, Rhode*
453 *Island, USA, August 10–15, 1986* (Vol. IV, pp. 221–224). Dordrecht: Springer
454 Netherlands.
- 455 Dietz, K.-J., Zörb, C., & Geilfus, C.-M. (2021). Drought and crop yield. *Plant Biology*, 23(6),
456 881–893.
- 457 Feddes, R. A., Kowalik, P., Kolinska-Malinka, K., & Zaradny, H. (1976). Simulation of field
458 water uptake by plants using a soil water dependent root extraction function. *Journal of*
459 *Hydrology*, 31(1), 13–26.

460 Grossiord, C., Buckley, T. N., Cernusak, L. A., Novick, K. A., Poulter, B., Siegwolf, R. T. W., et
461 al. (2020, June 1). Plant responses to rising vapor pressure deficit. *New Phytologist*.
462 Blackwell Publishing Ltd. <https://doi.org/10.1111/nph.16485>

463 Hubbard, R. M., Ryan, M. G., Stiller, V., & Sperry, J. S. (2001). Stomatal conductance and
464 photosynthesis vary linearly with plant hydraulic conductance in ponderosa pine. *Plant,*
465 *Cell & Environment*, 24(1), 113–121.

466 IPCC Climate Change. (2013). The physical science basis. (*No Title*). Retrieved from
467 <https://cir.nii.ac.jp/crid/1371413280484207233>

468 Jiang, C., Guan, K., Pan, M., Ryu, Y., Peng, B., & Wang, S. (2020). BESS-STAIR: a framework
469 to estimate daily, 30m, and all-weather crop evapotranspiration using multi-source
470 satellite data for the US Corn Belt. *Hydrology and Earth System Sciences*, 24(3).
471 Retrieved from <https://www.osti.gov/biblio/1616269>

472 Kattge, J., Knorr, W., Raddatz, T., & Wirth, C. (2009). Quantifying photosynthetic capacity and
473 its relationship to leaf nitrogen content for global-scale terrestrial biosphere models.
474 *Global Change Biology*, 15(4), 976–991.

475 Kimm, H., Guan, K., Gentine, P., Wu, J., Bernacchi, C. J., Sulman, B. N., et al. (2020).
476 Redefining droughts for the U.S. Corn Belt: The dominant role of atmospheric vapor
477 pressure deficit over soil moisture in regulating stomatal behavior of Maize and Soybean.
478 *Agricultural and Forest Meteorology*, 287(August 2019), 107930.

479 Lei, F., Crow, W. T., Holmes, T. R. H., Hain, C., & Anderson, M. C. (2018). Global
480 Investigation of Soil Moisture and Latent Heat Flux Coupling Strength. *Water Resources*
481 *Research*, 54(10), 8196–8215.

482 Leuning, R. (1995). A critical appraisal of a combined stomatal-photosynthesis model for C3

483 plants. *Plant, Cell & Environment*, 18(4), 339–355.

484 Li, L., Yang, Z.-L., Matheny, A. M., Zheng, H., Swenson, S. C., Lawrence, D. M., et al. (2021).
485 Representation of plant hydraulics in the Noah-MP land surface model: Model
486 development and multiscale evaluation. *Journal of Advances in Modeling Earth Systems*,
487 13(4). <https://doi.org/10.1029/2020ms002214>

488 Li, Y., Ye, W., Wang, M., & Yan, X. (2009). Climate change and drought: a risk assessment of
489 crop-yield impacts. *Climate Research*, 39, 31–46.

490 Lin, Y.-S., Medlyn, B. E., Duursma, R. A., Prentice, I. C., Wang, H., Baig, S., et al. (2015).
491 Optimal stomatal behaviour around the world. *Nature Climate Change*, 5(5), 459–464.

492 Liu, Y., Kumar, M., Katul, G. G., Feng, X., & Konings, A. G. (2020). Plant hydraulics
493 accentuates the effect of atmospheric moisture stress on transpiration. *Nature Climate*
494 *Change*, 10(7), 691–695.

495 Manzoni, S., Vico, G., Porporato, A., & Katul, G. (2013). Biological constraints on water
496 transport in the soil–plant–atmosphere system. *Advances in Water Resources*, 51, 292–
497 304.

498 Medlyn, B. E., Duursma, R. A., Eamus, D., Ellsworth, D. S., Prentice, I. C., Barton, C. V. M., et
499 al. (2011). Reconciling the optimal and empirical approaches to modelling stomatal
500 conductance. *Global Change Biology*, 17(6), 2134–2144.

501 Miner, G. L., & Bauerle, W. L. (2019). Seasonal responses of photosynthetic parameters in
502 maize and sunflower and their relationship with leaf functional traits. *Plant, Cell &*
503 *Environment*, 42(5), 1561–1574.

504 Miner, G. L., Bauerle, W. L., & Baldocchi, D. D. (2017). Estimating the sensitivity of stomatal
505 conductance to photosynthesis: a review. *Plant, Cell & Environment*, 40(7), 1214–1238.

506 Mishra, A. K., & Singh, V. P. (2010). A review of drought concepts. *Journal of Hydrology*,
507 391(1), 202–216.

508 Mitter, E. (2017). Gridded Soil Survey Geographic (gSSURGO-10) Database for the
509 Conterminous United States - 10 meter. Retrieved from [https://agris.fao.org/agris-](https://agris.fao.org/agris-search/search.do?recordID=US2019X00961)
510 [search/search.do?recordID=US2019X00961](https://agris.fao.org/agris-search/search.do?recordID=US2019X00961)

511 Niu, G. Y., Yang, Z. L., Mitchell, K. E., Chen, F., Ek, M. B., Barlage, M., et al. (2011). The
512 community Noah land surface model with multiparameterization options (Noah-MP): 1.
513 Model description and evaluation with local-scale measurements. *Journal of Geophysical*
514 *Research, D: Atmospheres*, 116(D12), 1–19.

515 Novick, K. A., Biederman, J. A., Desai, A. R., Litvak, M. E., Moore, D. J. P., Scott, R. L., &
516 Torn, M. S. (2018). The AmeriFlux network: A coalition of the willing. *Agricultural and*
517 *Forest Meteorology*, 249, 444–456.

518 Novick, Kimberly A., Ficklin, D. L., Stoy, P. C., Williams, C. A., Bohrer, G., Oishi, A. C., et al.
519 (2016). The increasing importance of atmospheric demand for ecosystem water and
520 carbon fluxes. *Nature Climate Change*, 6(11), 1023–1027.

521 Oren, R., Sperry, J. S., Katul, G. G., Pataki, D. E., Ewers, B. E., Phillips, N., & Schäfer, K. V. R.
522 (1999). Survey and synthesis of intra- and interspecific variation in stomatal sensitivity to
523 vapour pressure deficit. *Plant, Cell & Environment*, 22(12), 1515–1526.

524 Palmer, W. C. (1965). *Meteorological Drought*. U.S. Department of Commerce, Weather
525 Bureau.

526 Paschalis, A., Fatichi, S., Zscheischler, J., Ciais, P., Bahn, M., Boysen, L., et al. (2020). Rainfall
527 manipulation experiments as simulated by terrestrial biosphere models: Where do we
528 stand? *Global Change Biology*, 26(6), 3336–3355.

529 Prentice, I. C., Liang, X., Medlyn, B. E., & Wang, Y.-P. (2015). Reliable, robust and realistic:
530 the three R's of next-generation land-surface modelling. *Atmospheric Chemistry and*
531 *Physics*, 15(10), 5987–6005.

532 Rogers, A., Medlyn, B. E., Dukes, J. S., Bonan, G., von Caemmerer, S., Dietze, M. C., et al.
533 (2017). A roadmap for improving the representation of photosynthesis in Earth system
534 models. *The New Phytologist*, 213(1), 22–42.

535 Sinclair, T. R., Tanner, C. B., & Bennett, J. M. (1984). Water-Use Efficiency in Crop
536 Production. *Bioscience*, 34(1), 36–40.

537 Sperry, J. S. (2000). *Hydraulic constraints on plant gas exchange* (Vol. 104).

538 Suyker, A. (2016a). FLUXNET2015 US-Ne1 Mead - irrigated continuous maize site [Data set].
539 FluxNet; University of Nebraska - Lincoln. <https://doi.org/10.18140/FLX/1440084>

540 Suyker, A. (2016b). FLUXNET2015 US-Ne2 Mead - irrigated maize-soybean rotation site [Data
541 set]. FluxNet; University of Nebraska - Lincoln. <https://doi.org/10.18140/FLX/1440085>

542 Trugman, A. T., Medvigy, D., Mankin, J. S., & Anderegg, W. R. L. (2018). Soil moisture stress
543 as a major driver of carbon cycle uncertainty. *Geophysical Research Letters*, 45(13),
544 6495–6503.

545 Venturas, M. D., Sperry, J. S., & Hacke, U. G. (2017, June 1). Plant xylem hydraulics: What we
546 understand, current research, and future challenges. *Journal of Integrative Plant Biology*.
547 Blackwell Publishing Ltd. <https://doi.org/10.1111/jipb.12534>

548 Yang, Y., Guan, K., Peng, B., Pan, M., Jiang, C., & Franz, T. E. (2021). High-resolution
549 spatially explicit land surface model calibration using field-scale satellite-based daily
550 evapotranspiration product. *Journal of Hydrology*, 596(September), 125730.

551 Yang, Z.-L., Niu, G.-Y., Mitchell, K. E., Chen, F., Ek, M. B., Barlage, M., et al. (2011). The

552 community Noah land surface model with multiparameterization options (Noah-MP): 2.
553 Evaluation over global river basins. *Journal of Geophysical Research*, 116(D12), 1–16.
554